

## Motional Coherence in Fluid Phospholipid Membranes

Maikel C. Rheinstädter,<sup>1,2,\*</sup> Jhuma Das,<sup>1</sup> Elijah J. Flenner,<sup>1</sup> Beate Brüning,<sup>2,3</sup> Tilo Seydel,<sup>2</sup> and Ioan Kosztin<sup>1</sup>

<sup>1</sup>*Department of Physics and Astronomy, University of Missouri-Columbia, Columbia, Missouri 65211, USA*

<sup>2</sup>*Institut Laue-Langevin, 6 rue Jules Horowitz, B.P. 156, 38042 Grenoble Cedex 9, France*

<sup>3</sup>*Institut für Röntgenphysik, Friedrich-Hund Platz 1, 37077 Göttingen, Germany*

(Received 24 July 2008; published 12 December 2008)

We report a high energy-resolution neutron backscattering study, combined with *in situ* diffraction, to investigate slow molecular motions on nanosecond time scales in the fluid phase of phospholipid bilayers of 1,2-dimyristoyl-sn-glycero-3-phosphatidylcholine. A cooperative structural relaxation process was observed. From the in-plane scattering vector dependence of the relaxation rates in hydrogenated and deuterated samples, combined with results from a 0.1  $\mu$ s long all-atom molecular dynamics simulation, it is concluded that correlated dynamics in lipid membranes occurs over several lipid distances, spanning a time interval from pico- to nanoseconds.

DOI: 10.1103/PhysRevLett.101.248106

PACS numbers: 87.16.dj, 83.85.Hf, 87.14.Cc, 87.15.ap

It is speculated that atomic and molecular motions in regions of biomolecular systems with strong local interactions are highly correlated on a certain range of time and length scales [1,2]. In proteins, intraprotein correlations are believed to be essential for their biological functioning, such as protein folding, domain motion, and conformational changes. Very recently, interprotein correlations in protein crystals and also membranes have been reported from experiment and simulation [3,4]. Experimental and computational effort has been invested to study collective molecular motions in phospholipid model membranes [5–8] to understand the possible impact on physiological and biological functions of the bilayers, such as transport processes [9], and eventually their implication on the function of membrane-embedded proteins. While fast (picosecond) propagating collective microscopic fluctuations in the plane of the bilayer can be understood as sound waves [10,11], the slow (nanosecond) in-plane mesoscopic fluctuations (undulations) are governed by the elasticity properties of the bilayers [12].

We studied dynamical modes at nearest neighbor distances of the lipid molecules using the neutron backscattering technique [13]. These modes are too fast to be accessed by x-ray photon correlation spectroscopy, and the lateral length scales involved are too small to be resolved by dynamic light scattering or the neutron spin-echo technique. Selective deuteration was used to discriminate relaxations due to collective molecular motions from relaxations arising from localized, single molecule excitations. In this Letter, we examine results of inelastic neutron scattering experiments that demonstrate the existence of slow coherent motion of lipid molecules in the fluid phase of phospholipid bilayers. From the in-plane scattering vector dependence ( $q_{\parallel}$ ) of the measured relaxation rates, combined with results of a 0.1  $\mu$ s long all-atom molecular

dynamics (MD) simulation, we find that the cooperative structural dynamics in lipid membranes occurs over several lipid distances, spanning a time interval from pico- to nanoseconds.

The experiments were carried out at the cold neutron backscattering spectrometer IN16 [14] at the Institut Laue-Langevin (ILL) with an energy resolution of about 0.9  $\mu$ eV FWHM ( $\lambda = 6.27$  Å). An energy transfer of  $-15 \mu\text{eV} < E < +15 \mu\text{eV}$  and a  $q$  range of  $0.43 \text{ \AA}^{-1} < q < 1.92 \text{ \AA}^{-1}$  were scanned, accessing time scales of  $0.28 \text{ ns} < t < 4.6 \text{ ns}$  and length scales of  $3.2 \text{ \AA} < d < 14.6 \text{ \AA}$ . A separate line of diffraction detectors allowed us to determine the bilayer structure *in situ*. Protonated (DMPC-h) and partially (acyl chain) deuterated 1,2-dimyristoyl-sn-glycero-3-phosphatidylcholine (DMPC-d54) was obtained from Avanti Polar Lipids. Highly oriented multilamellar membrane stacks of several thousands of lipid bilayers of DMPC were prepared by spreading a solution of typically 25 mg/ml of lipid in trifluoroethylene/chloroform (1:1) on 2" silicon wafers, followed by subsequent drying in vacuum and hydration from D<sub>2</sub>O or H<sub>2</sub>O vapor. Twenty such wafers (five for DMPC-h) separated by small air gaps were combined and aligned with respect to each other to create a “sandwich sample” consisting of several thousands of highly oriented lipid bilayers (total mosaicity about 0.5°). The deuterated (protonated) samples had a total mass of about 400 mg (100 mg) of lipid. The samples were mounted in a hermetically sealed aluminum container within a cryostat and hydrated from D<sub>2</sub>O or H<sub>2</sub>O vapor. By aligning the bilayer normal at 135° or 45° with respect to the incoming neutron beam, the momentum transfer could be placed in the plane of the bilayers ( $q_{\parallel}$ ) or perpendicular to the membranes ( $q_z$ ). The lamellar spacing of the DMPC sample was determined to  $d_z = 54$  Å at  $T = 30$  °C, which corresponds to a relative humidity of RH = 99.6% [15].

Four different samples (referred to as  $S1$ ,  $S2$ ,  $S3$ , and  $S4$ ) were prepared:

Sample	Bilayer	Hydration
$S1$	DMPC- $d54$	$D_2O$
$S2$	DMPC- $d54$	$H_2O$
$S3$	DMPC- $h$	$D_2O$
$S4$	DMPC- $h$	$H_2O$

Neutrons are scattered by the atomic nuclei, and each element intrinsically has nonzero coherent and incoherent scattering cross sections. In experiments, the different contributions can be enhanced with respect to each other, by, e.g., using different isotopes or selective deuteration. While in protonated samples the *incoherent* scattering is dominant and the time-autocorrelation function of individual scatterers is accessed, (partial) deuteration emphasizes the *coherent* scattering and probes the pair correlation function. By careful analysis of the scattering of all samples  $S1$ – $S4$ , it was possible to emphasize between the collective and self-motions in the underlying dynamics.

Figure 1 exemplarily depicts spectra measured at  $q_{\parallel} = 0.5$  and  $1.5 \text{ \AA}^{-1}$  for  $S1$  and  $S4$  at a temperature of  $T = 303 \text{ K}$ , in the fluid phase of the bilayers. A fast and a slow relaxation process were visible in the data, and data were therefore fitted using two Lorentzians and convoluted with the instrumental resolution. Because the faster process (the broad Lorentzian) could not be determined with sufficient accuracy, this Letter focuses on the slower relaxation process ( $\omega_1$ ).  $\omega_1$  might contain contributions from incoherent and coherent scattering. A quantitative determination of the coherent and incoherent relaxation rates would require purely coherent and purely incoherent scatterers or neutron polarization analysis (which has not yet been realized on a

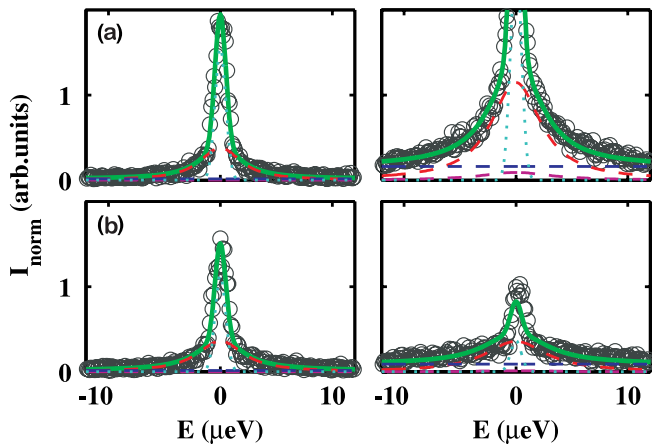


FIG. 1 (color online). Exemplary inelastic spectra in the fluid phase of the bilayers. Left column:  $q_{\parallel} = 0.5 \text{ \AA}^{-1}$ ; right column:  $q_{\parallel} = 1.5 \text{ \AA}^{-1}$ . (a) DMPC- $d54/D_2O$  (sample  $S1$ ); (b) DMPC- $h/H_2O$  (sample  $S4$ ). Data have been fitted using the instrumental resolution (dotted line), two Lorentzian peak shapes (red and magenta dashed lines), and a constant background (blue dashed line). The total fit is shown as a solid line.

neutron backscattering spectrometer) to discriminate the different contributions to  $\omega_1$ . A convolution of incoherent and coherent relaxation processes, each described by a Lorentzian peak shape (implicating a single exponential relaxation process), was assumed. Since the convolution of two Lorentzians with widths  $\Delta\omega_1'$  and  $\Delta\omega_1''$  is again a Lorentzian peak shape with a HWHM of  $\Delta\omega_1 = \Delta\omega_1' + \Delta\omega_1''$ , by subtracting the Lorentzian widths of spectra of protonated (mainly incoherent scatterers) from the (partially) deuterated samples (mainly coherent scatterers), it was qualitatively possible to distinguish the cooperative dynamics relative from the single-particle dynamics.

Figure 2(a) depicts in-plane diffraction patterns, i.e., structure factors  $S(q_{\parallel})$ , at 303 K. Subtracting  $S(q_{\parallel})$  for samples  $S3$  and  $S1$  emphasizes the coherent scattering of

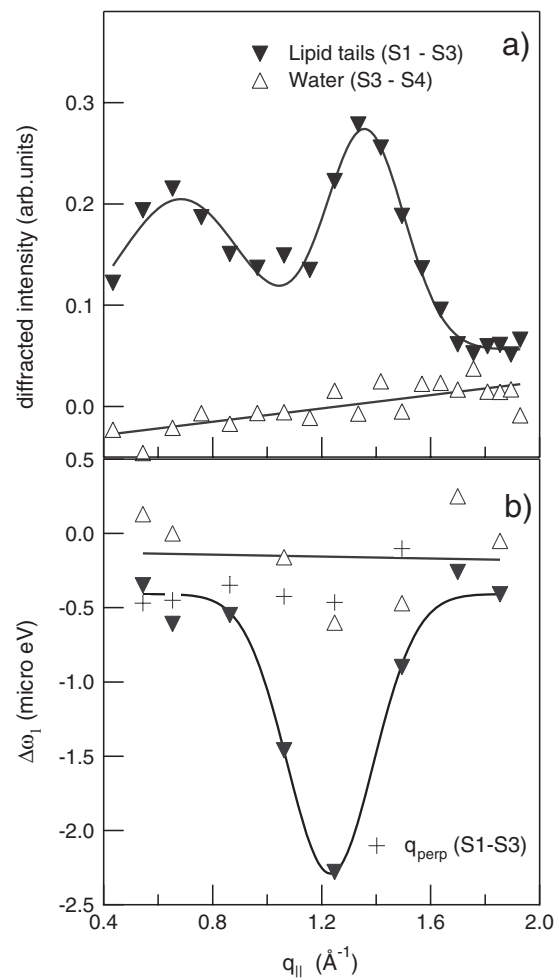


FIG. 2. (a) Diffraction patterns generated by subtraction of  $S(q_{\parallel})$  for pairs of samples  $S1$ – $S4$ , which emphasize contributions from collective motions of the lipid acyl chains ( $\blacktriangledown$ ) and the water molecules ( $\triangle$ ). See text for explanation. (b)  $\Delta\omega_1$  for the lipid acyl chains ( $\blacktriangledown$ ) and the membrane hydration water ( $\triangle$ ). For the water, the difference of  $\Delta\omega_1$  of samples  $S1$  and  $S2$  was taken. Peaks and minimum were fitted using Gaussian line shapes to determine position and width.

the lipid acyl chains. Finally, to emphasize coherent water scattering, the diffraction pattern of S4 was subtracted from that of S3. There are two peaks in  $S(q_{\parallel})$  of the lipid chains around  $q_{\parallel} = 0.7$  and  $1.4 \text{ \AA}^{-1}$ , which correspond to the nearest neighbor distances of phospholipid head groups and the acyl chains in DMPC, respectively. The water scattering is enhanced towards the water correlation peak around  $2 \text{ \AA}^{-1}$ , but there is no pronounced diffraction peak within the instrumental resolution.

Figure 2(b) shows the difference in the quasielastic width  $\Delta\omega_1(q_{\parallel})$  for the slow process for the lipid acyl chains and the membrane hydration water. So does, e.g., subtracting the widths of spectra S1–S3 emphasize the coherent lipid tail dynamics, analogous to the diffraction discussed above.  $\Delta\omega_1(q_{\parallel})$  shows a pronounced minimum around  $q_{\parallel} = 1.22 \text{ \AA}^{-1}$  for the lipids and qualitatively reproduces the behavior of  $S(q_{\parallel})$  in Fig. 2(a). This points to a strong coupling of dynamical properties to the static structure of the system and to a softening of the coherent relaxation rate around the maximum of the static structure factor  $S(q_{\parallel})$ . The slowing down of the decay of the density autocorrelation function for distances corresponding to nearest neighbors is known as *de Gennes narrowing* [16]. The momentum dependence of the dynamical parameters in the collective dynamics case is not trivial as in the single-particle case but points to coherent structural relaxation. Because the out-of-plane component ( $q_z$ ) of the scattering vector [also in Fig. 2(b)] shows no minimum, it is concluded that the relaxation process is confined to the plane of the membranes.

To gain further insight in the above relaxation process, we performed an all-atom MD simulation of DMPC and analyzed the motion of the carbons within the lipid tails. The fully solvated system, built from a preequilibrated DMPC bilayer [17], contained 128 lipid and 2577 water molecules. The MD simulation was performed with NAMD-2.6 [18] using the CHARMM27 [19] force field. The pair interactions were turned off smoothly from 10 to 12  $\text{\AA}$ , and the long-range electrostatic interactions were calculated using the particle-mesh Ewald method [20]. The simulation was performed in the *NVT* ensemble using periodic boundary conditions, with a simulation box of  $62 \times 62 \times 58.5 \text{ \AA}^3$ . A constant temperature of  $T = 303 \text{ K}$  was maintained by employing a Langevin thermostat with a coupling constant of  $0.05 \text{ ps}^{-1}$ . After proper energy minimization and thermal equilibration, a production run of  $0.1 \text{ \mu s}$  was carried out on 40 CPUs of a dual core 2.8 GHz Intel Xeon EM64T cluster with a performance of  $0.2 \text{ day/ns}$ .

To examine the structural relaxation of the lipid tails, we calculated the in-plane incoherent (self)  $I_s(q_{\parallel}, t) = (1/N) \sum_n \langle e^{-i\vec{q}_{\parallel} \cdot [\vec{r}_n(0) - \vec{r}_n(t)]} \rangle$  and the coherent  $I_c(q_{\parallel}, t) = (1/N) \sum_n \sum_m \langle e^{-i\vec{q}_{\parallel} \cdot [\vec{r}_n(0) - \vec{r}_m(t)]} \rangle$  intermediate scattering functions. The sums are taken over the  $N$  carbon atoms in the lipid tails, and  $\vec{r}_n(t)$  is the position of the  $n$ th atom at

time  $t$ . The scattering vector  $\vec{q}_{\parallel}$  is parallel to the  $x$ - $y$  plane of the lipid bilayer. By examining  $I_{s/c}(q_{\parallel}, t)$ , we can isolate purely coherent and incoherent contributions to the scattering due to the carbons within the lipid tails.

The minimum in  $\Delta\omega_1(q_{\parallel})$  shown in Fig. 2 suggests a longer relaxation time for  $I_c(q_{\parallel}, t)$  than for  $I_s(q_{\parallel}, t)$  for  $q_{\parallel}$  values around the peak of  $S(q_{\parallel}) = I_c(q_{\parallel}, 0)$ . Shown in the inset in Fig. 3 are  $I_{s/c}(q_{\parallel}, t)$  for  $q_{\parallel} = 2.5$  and  $1.42 \text{ \AA}^{-1}$ . For  $q_{\parallel} = 2.5 \text{ \AA}^{-1}$  the decay times for  $I_s(q_{\parallel}, t)$  and  $I_c(q_{\parallel}, t)$  are almost identical, but  $I_c(q_{\parallel}, t)$  decays slower for  $q_{\parallel}$  around the first peak of the static structure factor. We defined the decay time  $\tau(q_{\parallel})$  as when  $I_{s/c}(q_{\parallel}, \tau(q_{\parallel}))/I_{s/c}(q_{\parallel}, 0) = e^{-1}$ . Shown in Fig. 3 are  $\tau_s(q_{\parallel})$  and  $\tau_c(q_{\parallel})$  along with  $S(q_{\parallel})$ . Note that the nonmonotonic behavior of  $\tau_c(q_{\parallel})$  yields a minimum in the difference  $\tau_s - \tau_c$  around the peak of  $S(q_{\parallel})$ . Thus, the MD simulation results are in qualitative agreement with those from the experiment and reinforces the conclusion that the difference of the quasielastic widths  $\Delta\omega_1(q_{\parallel})$  is due to correlated dynamics of the lipid acyl chains.

To determine the temporal and spatial extent of the correlated motion of the lipid tails, we calculated the correlation function

$$g_{\Delta}(r, t) = \frac{V}{\langle \Delta r \rangle^2 N} \sum'_{n,m} \langle \Delta r_n(t) \Delta r_m(t) \rangle \times \delta(r - |\vec{r}_n(0) - \vec{r}_m(0)|),$$

where  $\Delta r_n(t) = |\vec{r}_{n,\parallel}(t) - \vec{r}_{n,\parallel}(0)|$  represents the displacement of carbon atoms in the  $x$ - $y$  plane of the membrane and the prime denotes a restricted double sum in which carbon pairs belonging to the same lipid tail are excluded. In

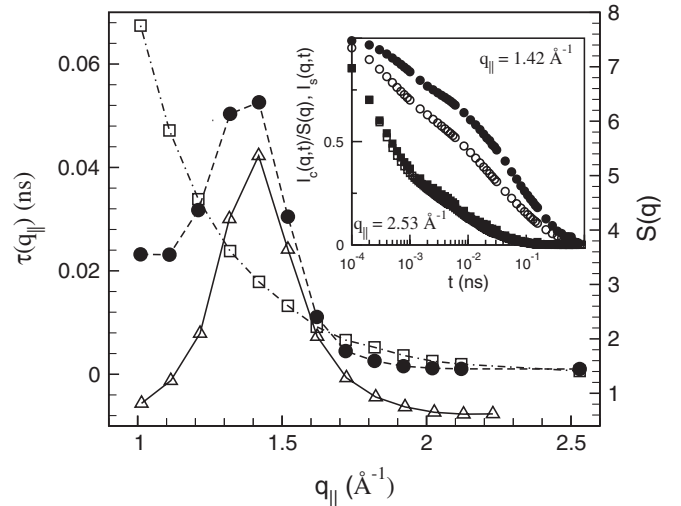


FIG. 3. The slow relaxation times  $\tau_c$  (solid circles) and  $\tau_s$  (open squares) as a function of wave vector  $q_{\parallel}$ . Also shown is the static structure factor  $S(q_{\parallel})$  (open triangles). Inset:  $I_s(q, t)$  (open symbols) and  $I_c(q, t)$  (solid symbols) for  $q_{\parallel} = 2.53$  (lower curves) and  $1.42 \text{ \AA}^{-1}$  (upper curves).

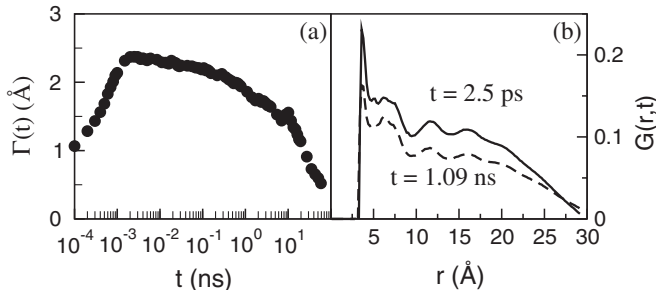


FIG. 4. Measures of the correlated dynamics  $\Gamma(t) = \int G(r, t) dr$ .  $\Gamma(t)$  is a measure of the size of the correlated displacement at a time  $t$ , and  $G(r, t)$  measures the spatial range of the correlations.

the absence of displacement correlations,  $g_{\Delta}(r, t) = g_1(r) = (V/N^2) \langle \sum'_{n,m} \delta(r - |\vec{r}_n - \vec{r}_m|) \rangle$ . Thus  $\Gamma(t) = \int [g_{\Delta}(r, t)/g_1(r) - 1] dr$  provides a measure of the correlation of in-plane displacements of the carbon atoms within the lipid tails between different lipids [21].

Examination of  $\Gamma(t)$  [Fig. 4(a)] shows that the displacements of the lipid acyl tails are correlated for times from around 1 ps to 10 ns, i.e., for much longer than the microscopic collision time but shorter than the time needed for a lipid to diffuse one lipid diameter. This is exactly the time window of the structural relaxation probed by the neutron scattering experiments and corresponds to the decay times  $\tau_{s/c}$ . Thus, we associate  $\Delta\omega_1$  observed in the experiments and the difference in decay times  $\tau_c - \tau_s$  to correlated motion of lipid tails.

Finally, the spatial decay of  $G(r, t) = g_{\Delta}(r, t)/g_1(r) - 1$  yields the length scale associated with the correlated displacements. Shown in Fig. 4(b) is  $G(r, t)$  for  $t_1 = 2.5$  ps [at the peak of  $\Gamma(t)$ ] and  $t_2 = 1.1$  ns. For both times,  $G(r, t)$  does not decay to zero until around 30 Å. Therefore, the lipid tails displacements are correlated for at least four lipid diameters between  $t_1$  and  $t_2$ .

In conclusion, we found experimental evidence for a cooperative structural relaxation process in fluid phospholipid membranes. An all-atom molecular dynamics simulation demonstrated that the displacements of the lipid tails are correlated for up to four lipid diameters for a time span from picoseconds to around ten nanoseconds. A possible implication of this motional coherence of the lipid acyl chains is, e.g., that information about a local structural perturbation of the lipids could propagate in the bilayer, which might be relevant for the understanding of processes and functions involving collective structural changes.

We acknowledge financial support from the DFG through Project No. SA 772/8-2. We thank T. Salditt

(Göttingen) for continuous support, E. Kats for critical reading of the manuscript and valuable comments, and the ILL for the allocation of beam time. Computer time was generously provided by the University of Missouri Bioinformatics Consortium.

\*RheinstadterM@missouri.edu

- [1] C.L. Brooks, M. Karplus, and B.M. Pettit, *Proteins: A Theoretical Perspective of Dynamics, Structure and Thermodynamics* (Wiley, New York, 1989).
- [2] *Structure and Dynamics of Membranes*, edited by R. Lipowsky and E. Sackmann, Handbook of Biological Physics Vol. 1 (Elsevier, Amsterdam, 1995).
- [3] V. Kurkal-Siebert, R. Agarwal, and J.C. Smith, Phys. Rev. Lett. **100**, 138102 (2008).
- [4] M.C. Rheinstädter, K. Schmalzl, K. Wood, and D. Strauch, arXiv:0803.0959.
- [5] T. Bayerl, Curr. Opin. Colloid Interface Sci. **5**, 232 (2000).
- [6] M.C. Rheinstädter, T. Seydel, W. Häußler, and T. Salditt, J. Vac. Sci. Technol. A **24**, 1191 (2006).
- [7] J.S. Hub, T. Salditt, M.C. Rheinstädter, and B.L. de Groot, Biophys. J. **93**, 3156 (2007).
- [8] M. Tarek, D.J. Tobias, S.-H. Chen, and M.L. Klein, Phys. Rev. Lett. **87**, 238101 (2001).
- [9] S. Paula, A.G. Volkov, A.N. Van Hoek, T.H. Haines, and D.W. Deamer, Biophys. J. **70**, 339 (1996).
- [10] S.-H. Chen, C.Y. Liao, H.W. Huang, T.M. Weiss, M.C. Bellisent-Funel, and F. Sette, Phys. Rev. Lett. **86**, 740 (2001).
- [11] M.C. Rheinstädter, C. Ollinger, G. Fragneto, F. Demmel, and T. Salditt, Phys. Rev. Lett. **93**, 108107 (2004).
- [12] M.C. Rheinstädter, W. Häußler, and T. Salditt, Phys. Rev. Lett. **97**, 048103 (2006).
- [13] M.C. Rheinstädter, T. Seydel, and T. Salditt, Phys. Rev. E **75**, 011907 (2007).
- [14] B. Frick and M. Gonzalez, Physica (Amsterdam) **301B**, 8 (2001).
- [15] N. Chu, N. Kücerka, Y. Liu, S. Tristram-Nagle, and J.F. Nagle, Phys. Rev. E **71**, 041904 (2005).
- [16] P.G. DeGennes, Physica (Amsterdam) **25**, 825 (1959).
- [17] A.A. Gurtovenko, M. Patra, M. Karttunen, and I. Vattulainen, Biophys. J. **86**, 3461 (2004).
- [18] J.C. Phillips, R. Braun, W. Wang, J. Gumbart, E. Tajkhorshid, E. Villa, C. Chipot, R.D. Skeel, L. Kale, and K. Schulten, J. Comput. Chem. **26**, 1781 (2005).
- [19] S.E. Feller and A.D. MacKerell, Jr., J. Phys. Chem. B **104**, 7510 (2000).
- [20] U. Essmann, L. Perera, M.L. Berkowitz, T. Darden, H. Lee, and L.G. Pedersen, J. Chem. Phys. **103**, 8577 (1995).
- [21] C. Bennemann, C. Donati, J. Baschnagel, and S.C. Glotzer, Nature (London) **399**, 246 (1999).